AIMS Energy, 11(5): 753–773.
DOI: 10.3934/energy.2023037
Received: 11 July 2023
Revised: 24 August 2023
Accepted: 27 August 2023
Published: 12 September 2023

http://www.aimspress.com/journal/energy

Research article

A novel design and simulation of a mechanical coordinate based photovoltaic solar tracking system

Sabir Rustemli[1], Zeki İlcihan[1], Gökhan Sahin[2,*] and Wilfried G. J. H. M. van Sark[2]

[1] Engineering Faculty, Electronical and Electronic Engineering Department, Bitlis Eren University, Bitlis, Turkey
[2] Copernicus Institute of Sustainable Development, Utrecht University, Princetonlaan 8A, 3584 CB Utrecht, The Netherlands

*** Correspondence:** Email: g.sahin@uu.nl.

Abstract: Various methods have been developed to increase electrical energy production gains in photovoltaic (PV) systems. These can be classified as solar tracking systems, cooling systems and methods of reducing the effect of shading. In order to maximise the PV energy yield, the PV systems must follow the sun. In this study, the effect of solar tracking systems on the energy yield gains of PV systems is investigated, and various types of solar tracking systems are discussed in detail. To ensure accuracte tracking of the postion of the sun, a new, low-cost, system has been developed that employs a global positioning system (GPS) module, compass and accelerometer. With this necessary angle information a dual-axis coordinate-based solar tracking system was designed using the Arduino Mega 2560 microcontroler with home-built control software. The system is validated by comparing it to a fixed angle system and an energy yield gain of 33–38% is found.

Keywords: solar energy; photovoltaic systems; solar tracking systems; yield enhancement; incidence angles

1. Introduction

With continued economic growth, electrical energy demand is increasing by approximately 4–8% every year [1,2]. Fossil fuel reserves, which meet a large part of the increasing electrical energy needs, will be depleted in the near future and therefore cannot meet the need [3,4]. Hence, new energy sources

are being developed that should meet the electrical energy needs in a way that will not harm humanity and the environment, i.e., renewable energy sources. One of the most useful resources among renewable energy sources is solar energy [5,6]. Many energy scenarios foresee solar to be the main pillar for a 100% renewables society [7]. Initially, solar energy was mostly used to produce hot water. Obtaining electrical energy directly from solar energy is provided by photovoltaic cells, which are combined in PV solar panels, and many panels are combined in solar arrays.

Various methods have been developed to increase electrical energy yield in photovoltaic panels. These methods are solar tracking systems, panel cooling systems and methods of reducing the effect of shading [8]. In order to keep solar intensity at the highest level at all hours of the day, PV panels must follow the sun. One of the most effective ways to improve energy yield is tracking the sun. If the panel surface is kept perpendicular to the incident angle of sun rays at all hours of the day, conversion efficiency is the highest and as a consequence, daily energy yield is maximized [9,10] compared to PV systems with fixed orientation and tilt.

Thanks to the solar tracking system, it is possible to benefit from the solar energy throughout the day and the lost part can be reintroduced into the system and the efficiency will increase solar tracking (solar tracker) systems may increase efficiency up to 40% [11–17]. The first solar tracking system was designed entirely mechanically at Valparaiso, Chile, by Finsher in 1962 and electronic control was added later by Saavedra, as described by Georgiev et al. [18].

In a review authored by Fuentes-Morales et al. [19], it was concluded that the most widely used sun tracking control strategy is closed loop, which represents about 54% of all referenced publications. The most applied control algorithms in active solar tracking systems are on-off, fuzzy logic, proportional-integral-derivative and proportional-integral control, which represent about 57%, 11%, 6% and 4%, respectively. Sharaf et al. [20] reviewed cooling techniques for PV systems. Today, the most used techniques are passive cooling (air ducts, heat sinks), active cooling with water or air and cooling with phase change materials (PCMs), which may lead to about 20% maximum yield enhancement. In a study of Golroodbari et al. [21], the non-linear effect of partial shading on the performance of photovoltaic (PV) modules was studied. Different methods of optimizing energy harvesting under partial shading conditions have been proposed to reduce this nonlinear effect. A general model is developed by simulating the behavior of smart architecture under different shading models. They reported that although the annual efficiency of the smart architecture is about 80% of the efficiency of an ideal module, the smart architecture outperforms a standard serial connected module by 47% and a parallel architecture by 13% [21].

In the axis tracking system study conducted by Chong et al. [22], the general coordinate transformation method was used to derive general sun-tracking equations. In this study, it has been proven that small errors of about 0.4% can lead to limits in energy gains [22]. In a study by Sungur [23], a solar tracking system was used to maximize the performance of PV panels. They analyzed the energy gain of fixed system and mobile solar tracking systems. The mechanical control unit of this system made the position and performance measurements of the solar panel. As a result, they saw that there was a 42.6% energy gain compared to the single axis. In a review by Singh et al., it was emphasized that the cost will be reduced when mass production is started by increasing the number of panels [24]. In another review by Rodríguez-Gallegos et al. [25], PV systems were analyzed with solar tracking and fixed single-sided and double-sided (bifacial) solar panel systems. As a result of this analysis, they showed that the energy yield can be increased by 30–40%, where 30% can be reached using dual axis, monofacial PV panels and 40% with dual axis, bufacial PV panels.

Gerardo Garcia-Gil and Juan M. Ramirez propose the design and implementation of a sun tracker based on panoramic images taken by a fisheye camera. These angles position the solar tracker according to the sun's elevation angle and are fed by a microcontroller that uses a compass to set the azimuth angle [26]. In a study by Barbara Mendecka et al., they assessed the feasibility of using the mechanical work generated by volumetric expansion loops in a paraffin-based LHTES device for photovoltaic (PV) solar tracking purposes. Thus, we hypothesize a new paradigm for efficient integration between thermal and PV solar power plants [27]. Barbara Mendecka and colleagues conducted a study on the actual thermo-mechanical design of the integrated TES tracking system. The presented results open up interesting perspectives in the development of multifunctional LHTES devices as a viable solution to increase efficiency and reduce energy production. This affects installation costs and energy efficiency [28].

In the present study, a low-cost solar tracking system is designed, which ensures that the sun rays reaching the earth at all angles during the day are perpendicular to the PV panel. Two low-speed DC motors are used to provide the movement of this dual-axis solar tracking system. The microcontroller provides the motion control of the system by receiving the coordinate (latitude and longitude) and time (date and time) data using GPS, as well as the direction and angle information from the electronic compass and accelerometer, through dedicated software. By operating the system in the east-west axis, it is ensured that the sun follows the sun all day long. Operating the system in the north-south direction allows the system to follow the sun throughout the year. By comparing the designed system with a fixed angle system at optimal orientation and tilt for Turkey, we will demonstrate that the energy gain is higher by 33–38% compared to a fixed PV system.

2. Materials and methods

2.1. Mechanical system design

The designed coordinate based solar tracking system (CBSTS) is a tip-tilt dual-axis tracker (TTDAT) type. The design of the mechanical system was made using the solidworks design software [29]. A three-dimensional solid model picture of the designed system is given in Figure 1.

For the solar tracking system mechanical design, an aluminum composite panel was used for the upper body and vertical motor carrier as it is a light and hard material. This composite panel is a building material formed by covering both sides of a material called polyelite (a kind of plastic) with aluminum sheets. It is very easy to use and process and is preferred because it is very light. It has been tried to ensure that the designed mechanical system is exposed to a minimum level of load in cases where the two motors to be used are in motion and stationary. In addition, while the motors provide the movement of the system in the vertical and horizontal axis, it is ensured that the horizontal and vertical position of the tracking system do not change in the passive state (de-energized state). The motor, which will provide the vertical axis movement (2 in Figure 1), is provided with a screw feature. This screw will be tightened and loosened by the forward and backward movement of the motor, and the vertical axis movement of the PV panel will be provided with minimum energy. The motor, which will provide movement on the horizontal axis (5 in Figure 1), is made in the form of a box and the fixed part is fixed to the upper body, while the upper body is connected to the lower body with the motor shaft. In order not to overload the motor shaft, four caster wheels are mounted on the coupling surface of the lower body to the upper body. The load is distributed on these wheels, and the horizontal

axis motor is exposed to a minimum load. The vertical axis motor can move the PV panel between 0 and 90° in approximately 4 minutes. The horizontal axis motor, on the other hand, completes the 360° movement in about 15 seconds. The solar tracker has been manufactured in house, as shown in Figure 2. Further detailed component designs and photographs can be found in the Appendix A.

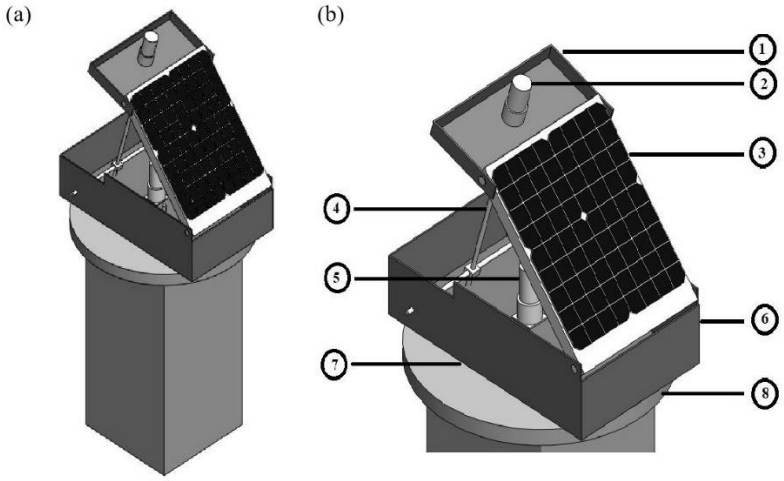

Figure 1. Three-dimensional solid model shape of the coordinate based solar tracking system. (a) overview; (b) details: 1) vertical drive motor carrier, 2) vertical motion motor, 3) PV panel, 4) vertical motion motor shaft, 5) horizontal motion motor, 6) upper body, 7) wheels carrying the upper body, 8) lower body (stand).

Figure 2. Manufactured system (left) tested in comparison with a fixed tilt system (right).

2.2. Electrical hardware

The electrical hardware consists of a PV panel, geared DC motors, a triple axis compass acceleration module LSM303, L298d motor driver module, GPS module, LCD Keypad module and Arduino Mega2560 microcontroller. Figure 3 shows the block diagram of electrical components.

Details of the circuit are shown in Figure C1. The 10 Wp commercial PV panel used consists of 4 monocrystalline silicon cells. Technical data are shown in Table 1. Maximum power voltage is typically 12 V in normal daylight, 10 V when the weather is overcast and 18 V under full sun.

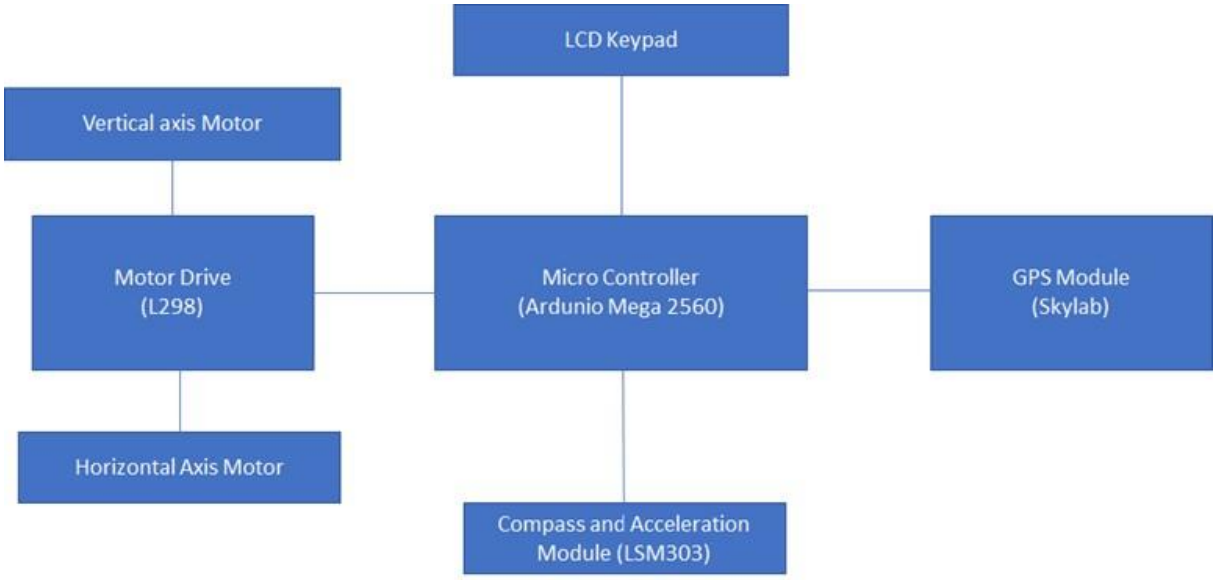

Figure 3. Block diagram of the electrical components in the system.

Table 1. PV panel technical specifications.

PV panel	Proporties
Specifications of panels	Monocrystalline silicon
Model	YLE10
Maximum power (P_{max}) (W)	10 W
Maximum power voltage (V_{mp})	18 V
Maximum power current (I_{mp})	0.56 A
Open circuit voltage (V_{oc})	21 V
Short circuit current (I_{sc})	0.66 A
Dimension	280 × 365 × 22 mm

2.3. Software control

For tracking the sun, the sun's position needs to be determined. Based on the information provided by the GPS unit, in combination with the date and time, the sun's position can be calculated. Our algorithm determines a horizontal (azimuth) angle and a vertical (elevation) angle reflecting daily and seasonal variations, as shown in Figure 4. It is based on the algorithm from Blanco-Muriel et al. [30]. We use the convention that North is 0°. A flow diagram is shown in Appendix D Figure D1.

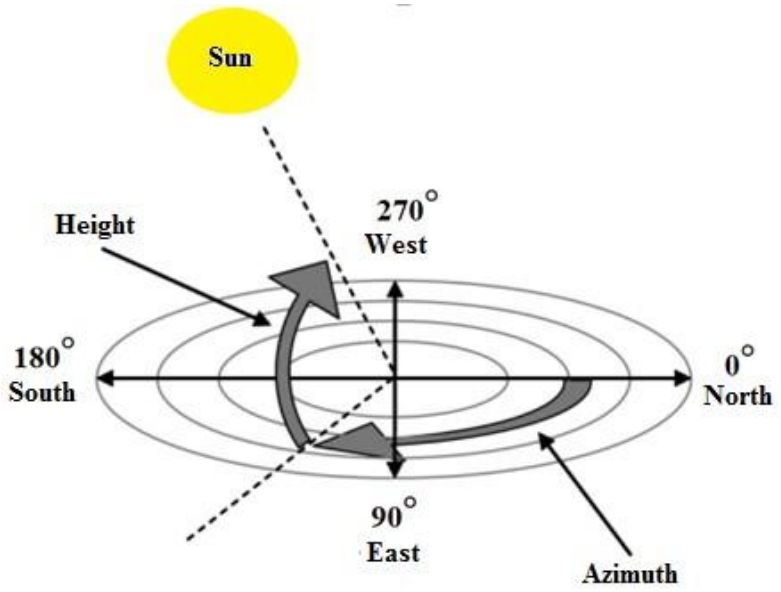

Figure 4. Relationship between elevation and azimuth angle.

After this calculation is done, our second step will be to bring the panel to these calculated angle values. In order to do this, we need to know the location information of the panel. LSM303 compass and acceleration module were used to learn the position information of the panel. This module is mounted parallel to the surface of the panel. First, calibration settings of the LSM303 module were made. Three angle values of the panel are taken from this module, whose calibration settings are made. These are pitch, roll and heading angles. Pitch value varies between 0 and 90° in our system. Heading indicates north at 0°, east at 90°, south at 180° and west at 270°.

Our next step is to drive the vertical and horizontal motors that will provide the movement to the solar tracking system mechanism. We will perform this operation using the L298 DC motor driver module. The Arduino Mega 2560 microcontroller compares the calculated height and azimuth angle values with the pitch and heading values found with the LSM303 module, determines which direction the vertical and horizontal motors will move and sends information to the L298 motor driver module accordingly. When the motors start to move, the motor movements continue until the values in the LSM303 module are equal to the calculated altitude and azimuth values. Figures D2 and D3 show the flow diagram for the motor control. Finally, the latitude, longitude, time and angle information are displayed on the LCD keypad module. We have created a menu section where we will determine how many minutes solar tracking system will follow during the day. Here, the desired information is displayed on the LCD screen by switching between the menus with the buttons on the LCD keypad module. The follow-up interval is set as 30 minutes and its multiples.

C programming language has been used and designed in the software of the solar tracking system. After compiling, the program was uploaded to the Arduino Mega 2560 microcontroller using Arduino IDE (integrated development environment). The control software includes drivers to all peripherals needed for the solar tracking system. The main program cycle starts after all peripherals are switched on and constantly calls functions, performs the task specified in the function content and leaves the main program. When the functions come back to the main program by affecting the state of a variable related to the peripheral unit they are related to, without leaving the main program, the value of this

variable will be learned and the operation will be performed. If the value of the variable has not changed, the function will not operate. If the value of the variable has changed, the operations for this situation will be performed. In this way, the system works faster by avoiding process redundancy.

2.4. Data acquisition

The experiment for the comparison of the designed solar tracking system and the fixed slope system was carried out in Muş province on the following day It was carried out on 21–24 June 2019, when the weather was clear, in a region receiving full sun. PV panels with the same characteristics were used in both systems. Tilt of the fixed tilt system angle was chosen equal to the latitude angle of the experimental setup. Load in both systems 47 Ω resistor with a power of 10 W was used. Current of both systems at five minute intervals and voltage values were measured and recorded with the data logger. As a result of the measurements on two different days, the movable PV panel was 33–38% higher than the fixed PV panel. increased earnings. For data acquisition a data logger was designed. It has two current and voltage inputs. It measures the voltage and current produced by two separate systems and saves them locally. The LCD screen on the data logger displays these values instantly. The data logger we used in the experimental study is shown in Figure C2.

3. Results

Two different approaches were followed to test the designed solar tracking system. First, the current and voltage values were compared by taking also measurements throughout the day with a fixed slope system (as shown in Figure 2). Second, the efficiency of the solar tracking system was calculated by measuring the shadow length of a stick placed on the photovoltaic panel.

3.1. Performance comparison

The experimental setup was established in the province of Muş in a region with a latitude of 38.753898 N and a longitude of 41.504688 E. In the fixed slope system, the PV panels slope is selected equal to the latitude angle. A 10 W 47 Ω resistor is used as a load resistor in solar tracking system. Voltage and current values measured at 5-minute intervals between 8:30 and 19:00 on 21 June 2019 and instantaneous power values were calculated. Results are shown in Figure 5.

From Figure 5, it is observed that at noon (12:00–13:30) the fixed system and solar tracking system voltage, current and power values are very close to each other and the solar tracking system voltage, current and power value are higher than the fixed system in the morning and evening hours. The current for the solar tracking system shows little change during most of the day, while it decreases substantially for the fixed system. This is similar for the power. The solar tracking system increased PV energy yield by 33.92% compared to the fixed system.

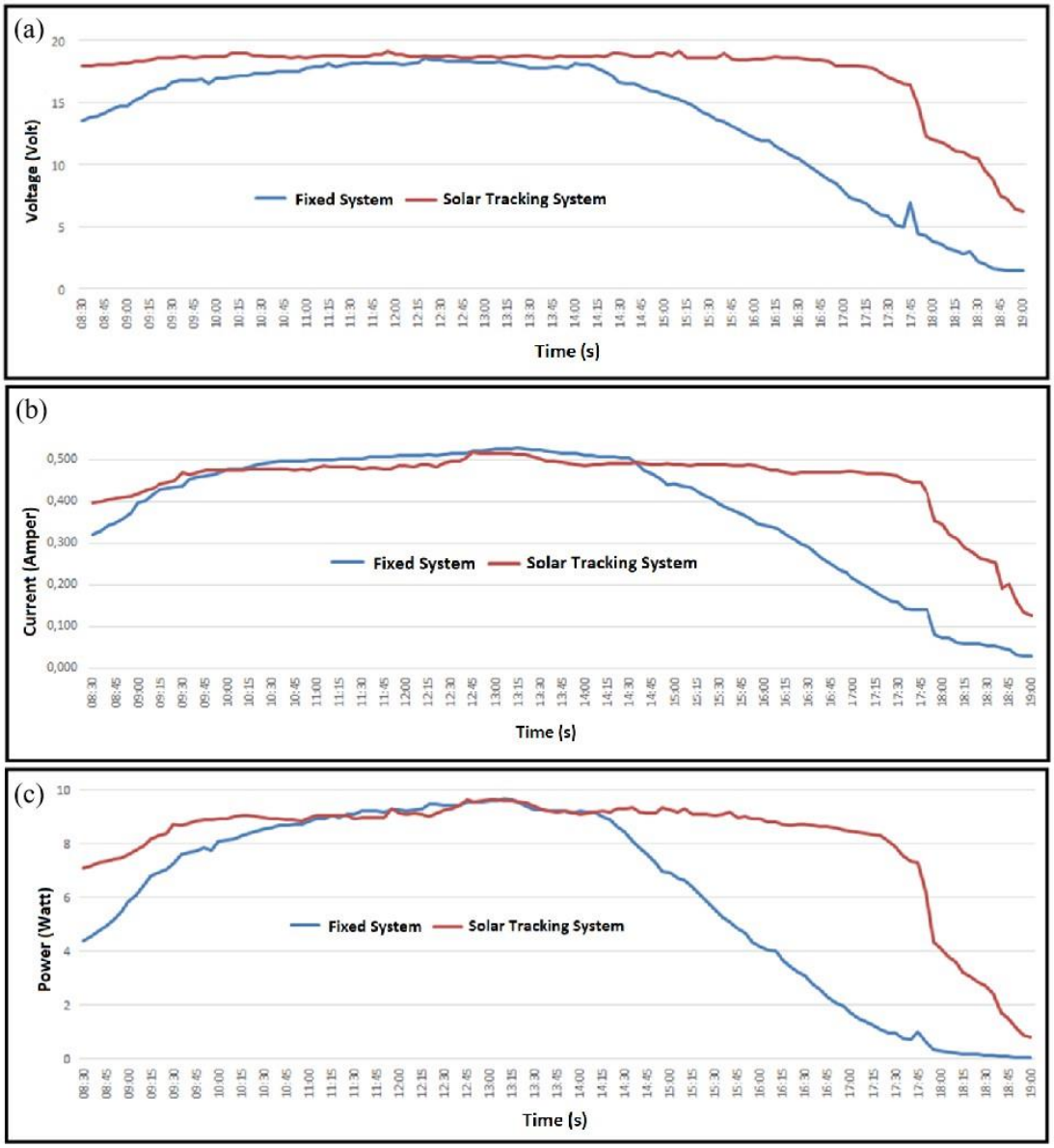

Figure 5. (a) Voltage, (b) current and (c) power measurements for the solar tracker system compared to the fixed tilt system on 21 June 2019.

The experiments were repeated on 24 June 2010, at 5-minute intervals between 8:00 and 19:00. Measured data are shown in Figure 6. When the test results on 24 June were examined, it was seen that the solar tracking system increased the PV panel gain by 38.2% compared to the fixed system, with the daily power values a little larger than the ones of 21 June.

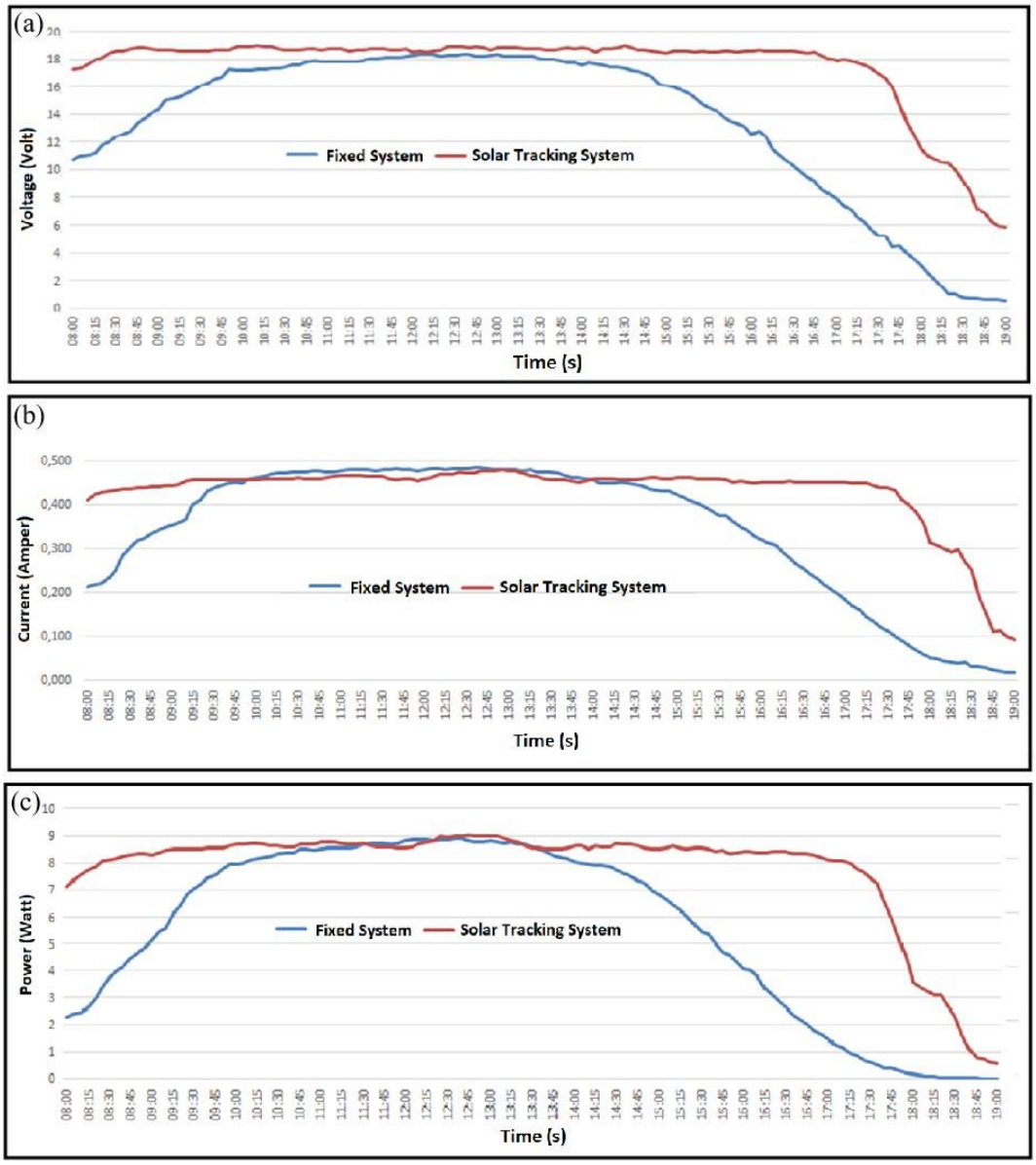

Figure 6. (a) Voltage, (b) current and (c) power measurements for the solar tracker system compared to the fixed tilt system on 24 June 2019.

3.2. Shadow length experiment

Two different applications were made with the designed solar tracking system. One of them was measured throughout the day with a fixed inclined system and the values were compared. The other one was measured with a rod placed on the PV panel and the shadow length was measured with a ruler and the efficiency of the designed solar tracking system was calculated. The efficiency and accuracy of the solar tracking system were experimentally determined by placing a rod perpendicular to the surface of the tracker, see Figure 7.

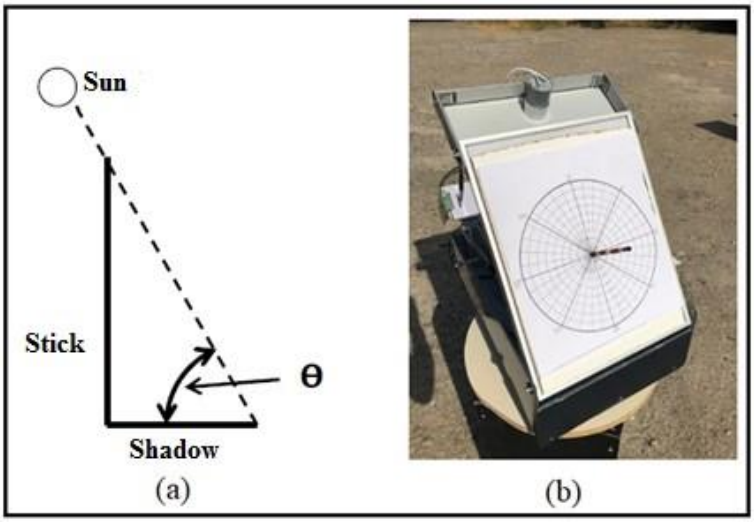

Figure 7. (a) Angle (θ) between stick and shadow (b) experimental setup.

Here, the angle between the stick and the shadow represents the solar incidence angles. When the solar tracking is perfect, this angle will be 90°. Thus, no shadow will be visible. The angle θ can be defined as follows:

$$\theta = tan^{-1}(\frac{L_B}{L_S}) \tag{1}$$

with L_B the length of the stick (mm) and L_S the shadows length (mm).

We then define the solar tracking system efficacy η_{STS} as

$$\eta_{STS} = \sin(\theta) \tag{2}$$

In this experimental study, the shadow lengths of the 10 cm long bar placed on the panel surface were measured and recorded with the measurements made at 30-minute intervals between 08:00 and 16:00 on July 1, 2019. The calculation shows that the solar tracking system efficiency was 0.9971 on average. In Table 2, shadow lengths measured at 30-minute intervals, calculated sun incidence angle and solar tracking system efficacy values are given. It is clear that around noon the highest efficacy values are found.

Table 2. Solar tracking system efficacy values.

Time (s)	Shadow length (mm)	θ (degree)	Efficiency% sin(θ)
08:00	12	83.16	0.9928
08:30	10	84.29	0.9950
09:00	8	85.43	0.9968
09:30	8	85.43	0.9968
10:00	9	84.86	0.9959
10:30	7	86.00	0.9975
11:00	4	87.71	0.9992
11:30	5	87.14	0.9987

Continued on next page

Time (s)	Shadow length (mm)	θ (degree)	Efficiency% sin(θ)
12:00	4	87.71	0.9975
12:30	4	87.71	0.9975
13:00	4	87.71	0.9975
13:30	5	87.14	0.9987
14:00	7	86.00	0.9975
14:30	6	86.57	0.9982
15:00	8	85.43	0.9968
15:30	9	84.86	0.9959
16:00	11	83.72	0.9939

4. Conclusions

In this study, an open-loop solar tracking system working with a tracking algorithm [30] was designed. It is ensured that the designed solar tracking system works automatically when it is active. Thus, the solar tracking system is able to track the sun to the PV panel wherever it is in the world, without the need for any external intervention. It has been observed by experimental studies on clear days that the designed solar tracking system increases the PV panel energy yield by 33–38% compared to the fixed PV panel on two different days. Another experiment in which a shadow was analyzed that was cast by placing a bar on top of the tracker, showed that the efficacy of tracking was very high. Due to the benefit to be gained from the use of this tracking system, it is certain that less panels will be used in solar-tracked PV systems and therefore solar-tracked PV will be used in proportion to the benefit obtained compared to systems using fixed panels.

Use of AI tools declaration

The author declare that the research was conducted and presented in this article have not used AI tools at all stages of the research process.

Acknowledgements

This article was written by Zeki İlcihan in Birlis Eren University, Institute of Science and Technology under the supervision of Prof. Dr. Sabir Rustemli. It is derived from Zeki İlcihan's master thesis entitled (Coordinate Based Solar Tracking System Design).

Conflict of interest

The authors declare no conflict of interest.

Author contributions

Sabir Rustemli: visualization, supervising, writing—review & editing, investigation part of solar energy power plant site selection; Zeki İlcihan: software, writing—review & editing, investigation of

solar energy power plant site selection; Gökhan ŞAHİN: software, writing—review & editing, investigation of solar energy power plant site selection; Wilfried G. J. H. M. van Sark: software, writing—review & editing, investigation of solar energy power plant site selection.

References

1. Hernández-Callejo L, Gallardo-Saavedra S, Alonso-Gómez V (2019) A review of photovoltaic systems: Design, operation and maintenance. *Sol Energy* 188: 426–440. https://doi.org/10.1016/j.solener.2019.06.017
2. Bouckaert S, Pales AF, McGlade C, et al. (2021) Net zero by 2050: A Roadmap for the global energy sector. International Energy Agency (IEA), Paris, France. Available from: https://www.iea.org/reports/net-zero-by-2050.
3. Anton SG, Nucu AEA (2020) The effect of financial development on renewable energy consumption. A panel data approach. *Renewable Energy* 147: 330–338. https://doi.org/10.1016/j.renene.2019.09.005
4. Zafar MW, Shahbaz M, Hou F, et al. (2019) From nonrenewable to renewable energy and its impact on economic growth: The role of research & development expenditures in Asia-Pacific economic cooperation countries. *J Cleaner Prod* 212: 1166–1178. https://doi.org/10.1016/j.jclepro.2018.12.081
5. Gielen D, Gorini R, Leme R, et al. (2021) World energy transitions outlook 1.5 ℃ pathway. International Renewable Energy Agency (IRENA), Abu Dhabi. Available from: https://www.irena.org/publications/2021/Jun/World-Energy-Transitions-Outlook.
6. European Commission (EC) (2018) A clean planet for all: A european strategic long-term vision for a prosperous, modern, competitive and climate neutral economy. Brussels, Belgium. Available from: https://eur-lex.europa.eu/legal-content/EN/TXT/PDF/?uri=CELEX:52018DC0773.
7. Breyer C, Khalili S, Bogdanov D, et al. (2022) On the history and future of 100% renewable energy systems research. *IEEE Access* 10: 78176–78218. https://doi.org/10.1109/ACCESS.2022.3193402
8. Rustemli S, Dincer F, Unal E, et al. (2013) The analysis on sun tracking and cooling systems for photovoltaic panels. *Renewable Sustainable Energy Rev* 22: 598–603. https://doi.org/10.1016/j.rser.2013.02.014
9. Eldin SAS, Abd-Elhady MS, Kandil HA (2016) Feasibility of solar tracking systems for PV panels in hot and cold regions. *Renewable Energy* 85: 228–233. https://doi.org/10.1016/j.renene.2015.06.051
10. Hafez A, Yousef AM, Harag NM (2018) Solar tracking systems: Technologies and trackers drive types—A review. *Renewable Sustainable Energy Rev* 91: 754–782. https://doi.org/10.1016/j.rser.2018.03.094
11. Batayneh W, Bataineh A, Soliman I, et al. (2019) Investigation of a single-axis discrete solar tracking system for reduced actuations and maximum energy collection. *Automat Constr* 98: 102–109. https://doi.org/10.1016/j.autcon.2018.11.011
12. Chin CS, Babu A, McBride W (2011) Design, modeling and testing of a standalone single axis active solar tracker using MATLAB/Simulink. *Renewable Energy* 36: 3075–3090. https://doi.org/10.1016/j.renene.2011.03.026

13. Yao Y, Hu Y, Gao S, et al. (2014) A multipurpose dual-axis solar tracker with two tracking strategies. *Renewable Energy* 72: 88–98. https://doi.org/10.1016/j.renene.2014.07.002
14. Fathabadi H (2016) Novel high accurate sensorless dual-axis solar tracking system controlled by maximum power point tracking unit of photovoltaic systems. *Appl Energy* 173: 448–459. https://doi.org/10.1016/j.apenergy.2016.03.109
15. Fathabadi H (2016) Comparative study between two novel sensorless and sensor based dual-axis solar trackers. *Sol Energy* 138: 67–76. https://doi.org/10.1016/j.solener.2016.09.009
16. Safan YM, Shaaban S, El-Sebah MIA (2018) Performance evaluation of a multi-degree of freedom hybrid controlled dual axis solar tracking system. *Sol Energy* 170: 576–585. https://doi.org/10.1016/j.solener.2018.06.011
17. Abdollahpour M, Golzarian MR, Rohani A, et al. (2018) Development of a machine vision dual-axis solar tracking system. *Sol Energy* 169: 136–143. https://doi.org/10.1016/j.solener.2018.03.059
18. Georgiev A, Roth P, Olıvares A (2004) Sun following system adjustment at the UTFSM. *Energy Convers Manage* 45: 1795–1806. https://doi.org/10.1016/j.enconman.2003.09.024
19. Fuentes-Morales RF, Diaz-Ponce A, Peña-Cruz MI, et al. (2020) Control algorithms applied to active solar tracking systems: A review. *Sol Energy* 212: 203–219. https://doi.org/10.1016/j.solener.2020.10.071
20. Sharaf M, Yousef MS, Huzayyin AS (2022) Review of cooling techniques used to enhance the efficiency of photovoltaic power systems. *Environ Sci Pollut Res* 29: 26131–26159. https://doi.org/10.1007/s11356-022-18719-9
21. Mirbagheri Golroodbari SZ, De Waal AC, Van Sark WG (2018) Improvement of shade resilience in photovoltaic modules using buck converters in a smart module architecture. *Energies* 11: 250. https://doi.org/10.3390/en11010250
22. Chong KK, Wong CW (2009) General formula for on-axis sun-tracking system and its application in improving tracking accuracy of solar collector. *Sol Energy* 83: 298–305. https://doi.org/10.1016/j.solener.2008.08.003
23. Sungur C (2009) Multi-axes sun-tracking system with PLC control for photovoltaic panels in Turkey. *Renewable Energy* 34: 1119–1125. https://doi.org/10.1016/j.renene.2008.06.020
24. Singh R, Kumar S, Gehlot A, et al. (2018) An imperative role of sun trackers in photovoltaic technology: A review. *Renewable Sustainable Energy Rev* 82: 3263–3278. https://doi.org/10.1016/j.rser.2017.10.018
25. Rodríguez-Gallegos CD, Liu H, Gandhi O, et al. (2020) Global techno-economic performance of bifacial and tracking photovoltaic systems. *Joule* 4: 1514–1541. https://doi.org/10.1016/j.joule.2020.05.005
26. Garcia-Gil G, Ramirez JM (2019) Fish-eye camera and image processing for commanding a solar tracker. *Heliyon* 5: e01398. https://doi.org/10.1016/j.heliyon.2019.e01398
27. Mendecka B, Di Ilio G, Krastev VK, et al. (2022) Technical assessment of phase change material thermal expansion for passive solar tracking in residential thermal energy storage applications. *J Energy Storage* 48: 103990. https://doi.org/10.1016/j.est.2022.103990
28. Mendecka B, Di Ilio G, Krastev VK, et al. (2022) Evaluating the potential of phase-change induced volumetric expansion in thermal energy storage media for passive solar tracking in high-temperature solar energy systems. *Appl Therm Eng* 212: 118561. https://doi.org/10.1016/j.applthermaleng.2022.118561

29. Solidworks design software program. Available from: https://www.solidworks.com.
30. Blanco-Muriel M, Alarcón-Padilla DC, López-Moratalla T, et al. (2001) Computing the solar vector. *Sol Energy* 70: 431–441. https://doi.org/10.1016/S0038-092X(00)00156-0

Appendix A

Details of component design are shown in Figures A1–A5.

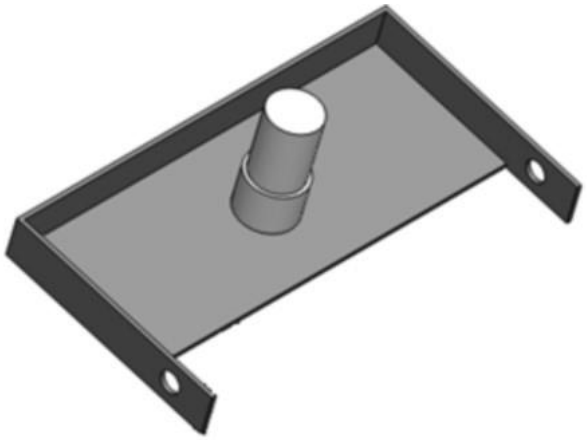

Figure A1. Vertical drive motor carrier.

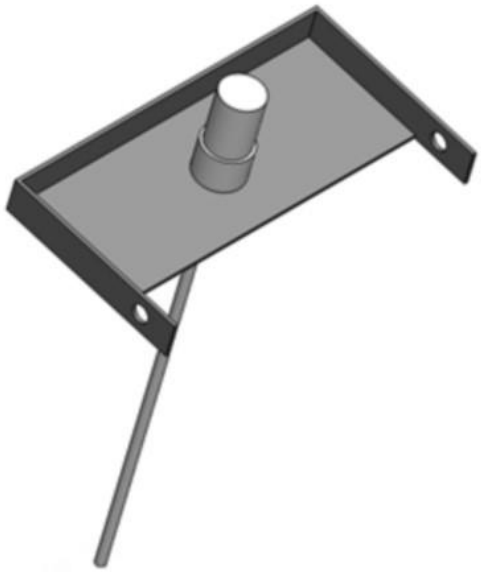

Figure A2. Vertical drive motor shaft.

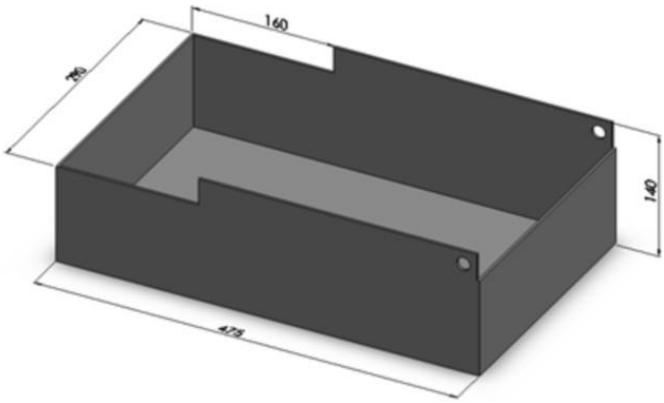

Figure A3. Upper body.

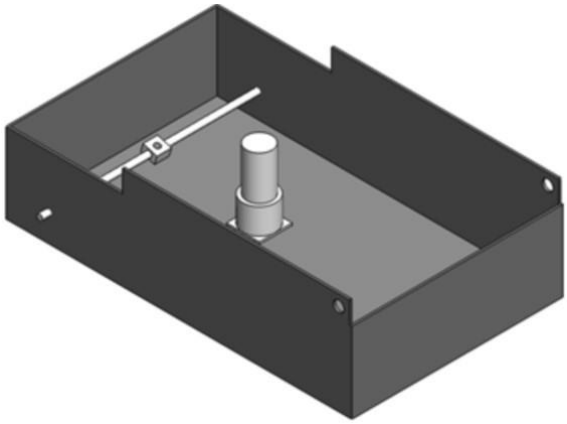

Figure A4. Upper body azimuth motor and vertical drive shaft bearing added.

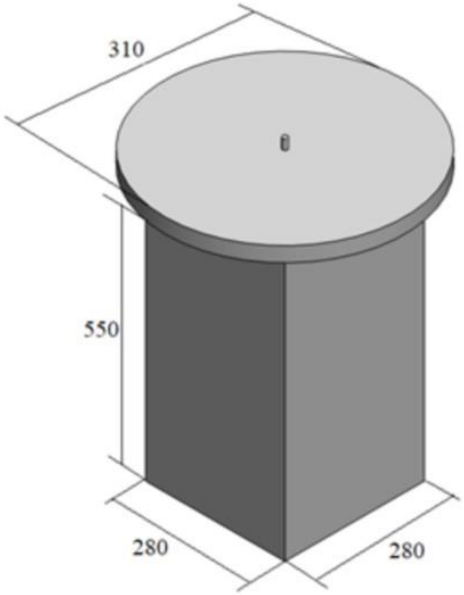

Figure A5. Lower body (stand).

Appendix B

Photographs of manufactured components are shown in Figures B1 and B2.

Figure B1. Various components assembly.

Figure B2. Full assembled tracker system.

Appendix C

Photographs and schematics of electronics components are shown in Figure C1.

Data recorded by the data logger is saved locally on the micro SD card. There is a DS3231 RTC (real time clock) module on the data logger, the time information received with this module is recorded on the micro SD card with the measured values. With the LCD screen on the data logger, the date, time and measured values are displayed instantly. At the end of the set time, the measured current and voltage information is recorded together with the time information in the desired recording interval and data recording is performed. Two ASC712-5A hall effect current sensors are used to measure

current. A voltage divider circuit with a potentiometer was used to measure the voltage. Since the current sensor can measure current in two directions, the value of 512 was subtracted from the measured value and the calculations were made with the Arduino Uno microcontroller. See Figure C2.

Figure C3 shows photographs of the solar tracker control unit in the field.

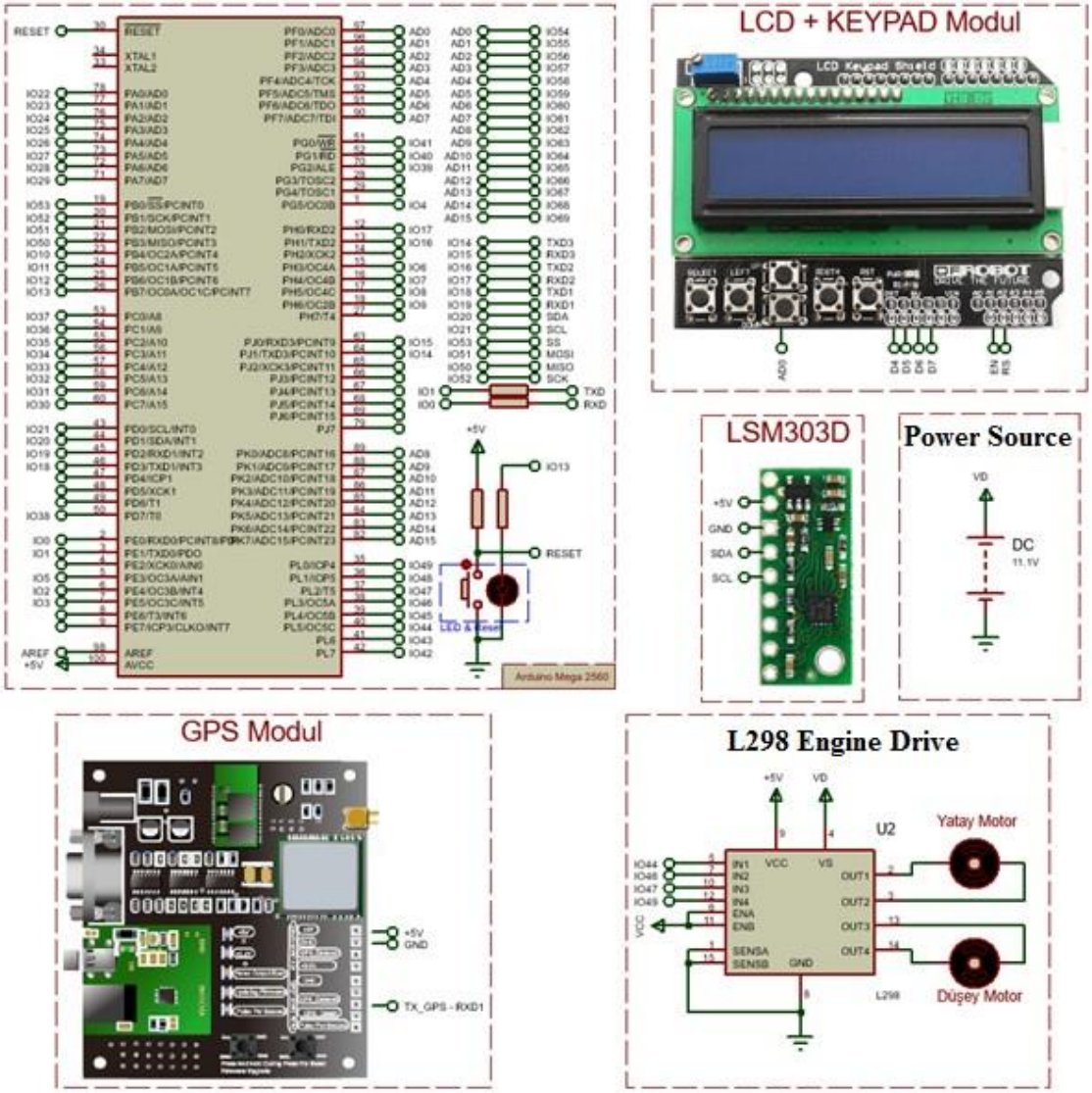

Figure C1. Solar tracking system control circuit.

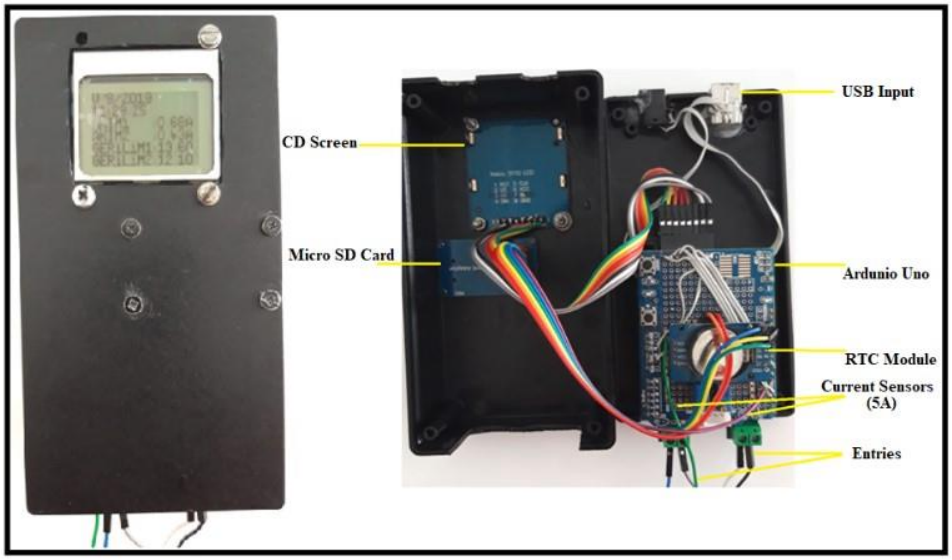

Figure C2. The data logger used in the experiment.

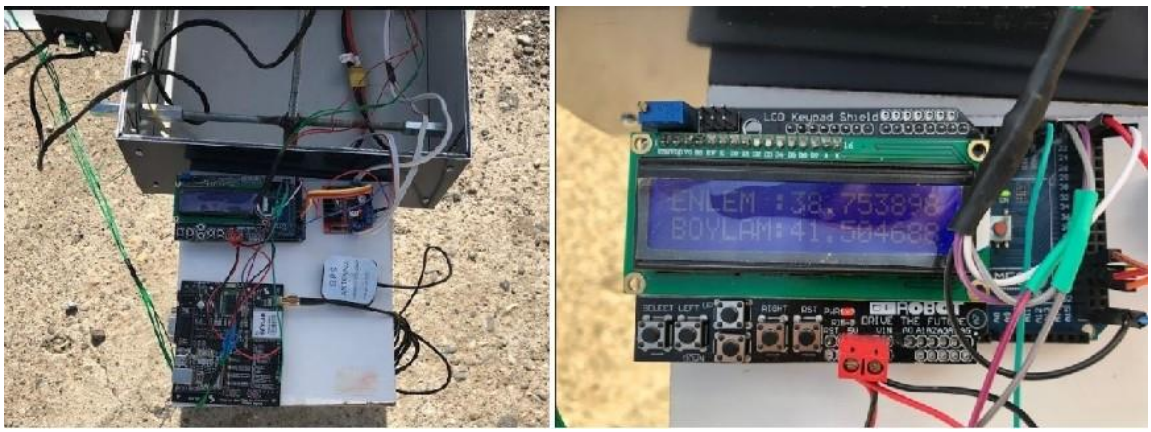

Figure C3. The controller at work in the field.

Appendix D

Flow diagrams of various algorithms.

The GPS module communicates with the microcontroller via a serial port. Time and location information from the GPS to the microcontroller comes in National Marine Electronics Association (NMEA) format with American Standard Code for Information Interchange (ASCII) characters. Incoming global positioning system information is loaded into a buffer until the end of line character [enter('\r')]. Then these NMEA codes in this buffer are decoded. From here, date time and latitude longitude information is obtained. Time information of the received information, date (day, month, year) and coordinated universal time information (hour, minute, second). Location information is in the form of six digits after the latitude and longitude degrees. Figure D1 shows the flow diagram of the global positioning system module.

The position angles of the sun are calculated from the location and time information from the GPS. The angles of the panel are calculated from the information from the accelerometer and compass sensor. Now that the angles are found, the vertical and horizontal motor is started until the vertical and horizontal angles are equal. L298 motor drive icloud (IC) is used to drive the motors. Two terminals are used in the motor driver to control each motor, these are Input1 (IN1) and Input2 (IN2) terminals. If one of these terminals is at logic 1 and the other is at logic 0, the motor rotates in one direction. If the sequence is changed, the motor will spin in the other direction. Since the rotational speed of the horizontal motor is very high, the speed of the motor is reduced by using pulse width modulation (PWM). Figure D2 shows the flow diagram of the vertical engine. Figure D3 shows the flow diagram of the horizontal engine.

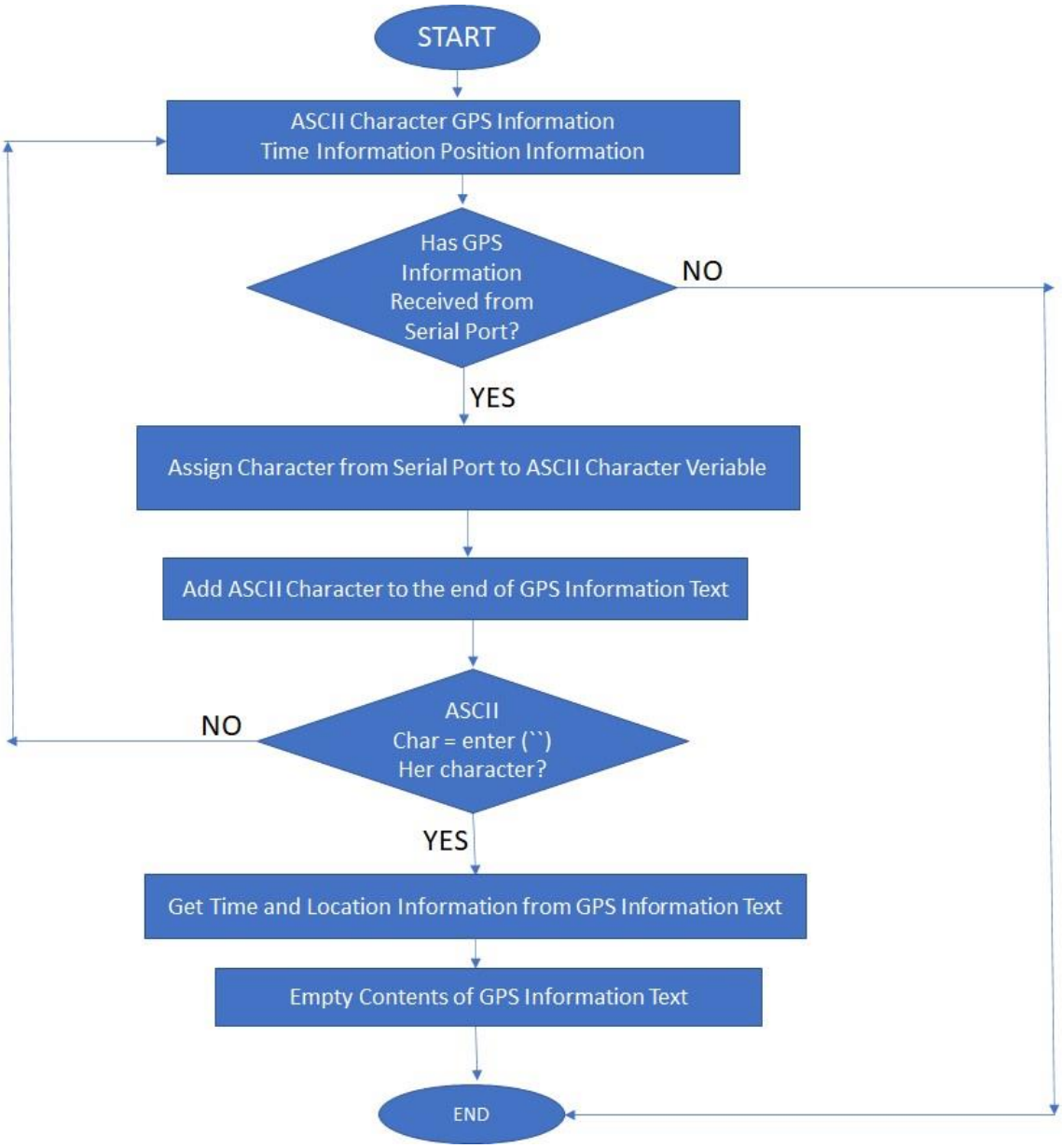

Figure D1. Flow diagram of the GPS module.

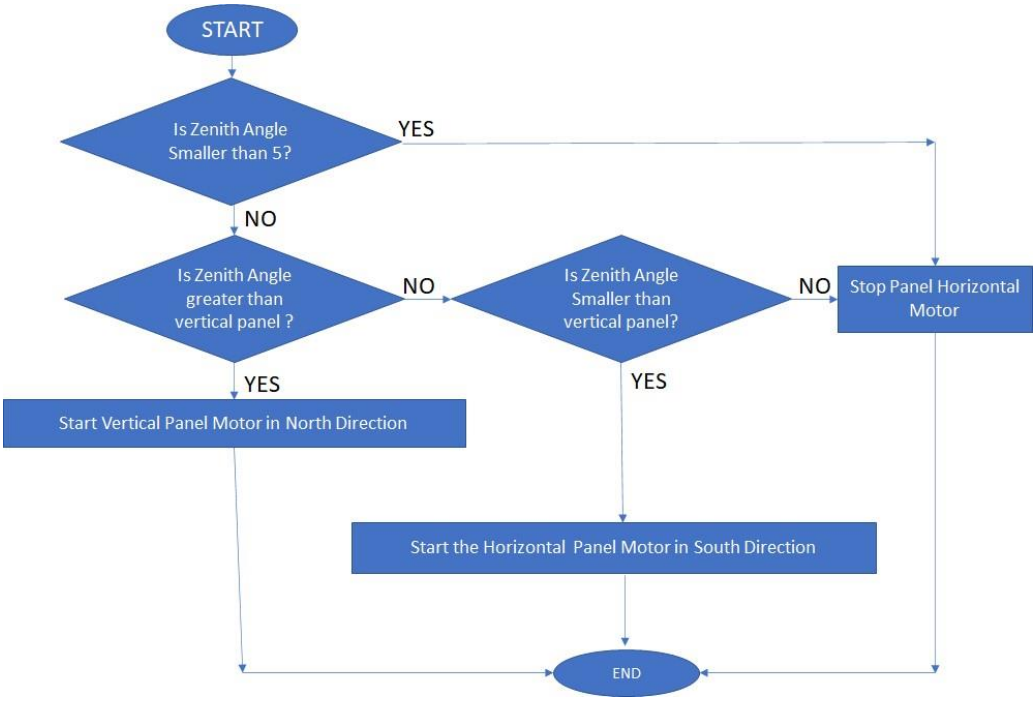

Figure D2. Flow diagram of vertical engine.

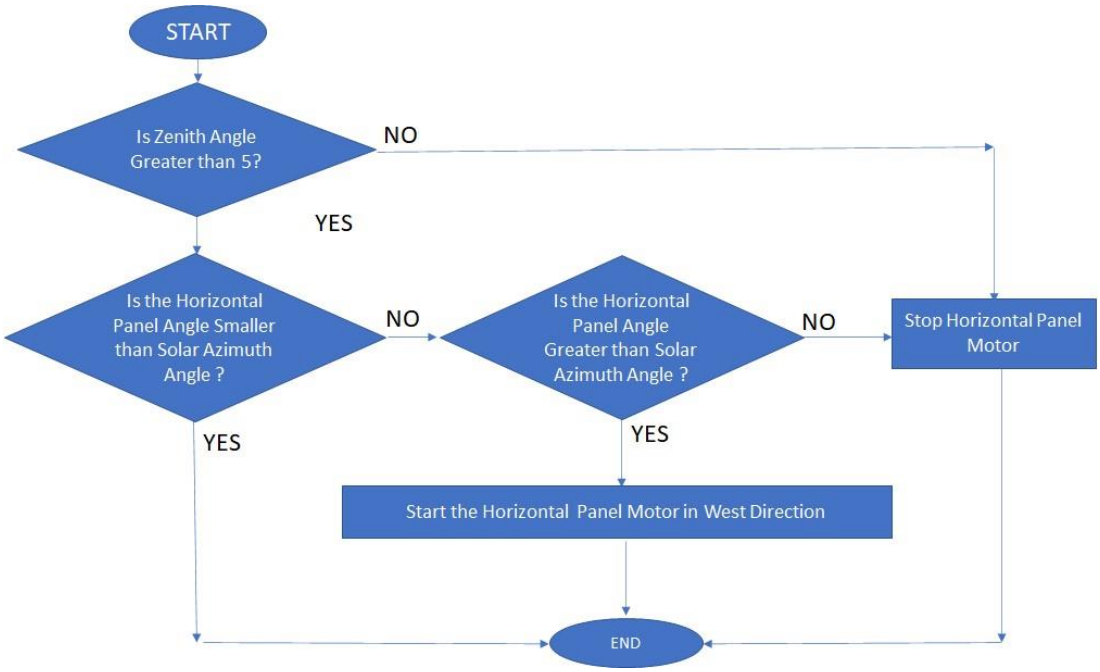

Figure D3. Flow chart of horizontal engine.